Protein Expression and Purification 148 (2018) 30–39

Contents lists available at ScienceDirect

Protein Expression and Purification

journal homepage: www.elsevier.com/locate/yprep

# A novel strategy to produce high level and high purity of bioactive IL15 fusion proteins from mammalian cells

Haomin Huang*,[2], Yuying Luo[1], Hanna Baradei[1], Shan Liu[1], Keneshia K. Haenssen[1], Supriya Sanglikar[1], Senthil Kumar, John Cini

*Sonnet Biotherapeutics, 1 Duncan Drive, Cranbury, NJ 08512, USA*

ARTICLE INFO

*Keywords:*
Interleukin 15
IL-15
Fusion protein
Protein production
Protein expression
Mammalian cell expression

ABSTRACT

IL15, a member of the common γ chain receptor (γc) cytokine family, is gaining attention in recent years as one of the most promising anti-tumor agents. IL15 regulates T cell activation and proliferation, promotes the survival of $CD8^+$ $CD44^{hi}$ memory T cells and is also essential for NK cell expansion and development. Despite the attraction of developing IL15 as an anti-cancer agent, production of recombinant IL15 has proven to be difficult due to the stringent control of IL15 expression at the transcriptional, translational and the post-translational levels. Furthermore, the bioactivity of IL15 fused to an extra functional domain that is isolated from mammalian cells is generally inferior to recombinant IL15 produced by *E. coli*. In this study, we report that Lysine 86 in IL15 is responsible for the instability in mammalian cells when its C-terminus is fused to the albumin binding scFv (IL15-A10m3). We demonstrate that K86A or K86R mutants increased the expression of the fusion protein from HEK293 cells. When the wild type IL15 is used for the fusion, no recombinant IL15 fusion was detected in the culture media. Additionally, we determined that the residue 112 in IL15 is critical for the bioactivity of IL15-A10m3. Examination of single and double mutants provides a better understanding of how IL15 engages with its receptor complex to achieve full signaling capacity. The results of our experiments were successfully applied to scale up production to levels up to 50 mg/L and > 10 mg/L of > 95% pure monomeric recombinant fusion proteins after a 2-step purification from culture media. More importantly, the recombinant fusion protein produced is fully active in stimulating T cell proliferation, when compared to the recombinant wild type IL15.

## 1. Introduction

Interleukin 15 (IL15) is a potent cytokine that regulates $CD8^+$ T cell and natural killer (NK) cell proliferation and development. Like IL2, IL15 belongs to the four α bundle cytokine family, where they interact with a trimeric receptor, containing the common γ receptor (γc), a shared β receptor (IL2-Rβ) and a specific α receptor (IL15Rα).

The IL2β receptor and γc complex is responsible for mediating signal transduction, via Jak-1/3 and STAT3/5 pathways [1]. Although IL15Rα does not appear to be essential for IL15 induced signal transduction, IL15Rα is believed to enhance the binding of IL15 to its receptor complex to facilitate downstream signaling in *trans* [2,3]. The crystal structures of the IL15 binary complex (IL15-IL15Rα) and quaternary complex (IL15-IL15Rα-IL2Rβ- γc) have been solved recently [4,5]. Helix C and helix D of the IL15 are involved in interactions with IL2-Rβ and γc receptors respectively. Consistent with the structural data, Asn65 and Asn72 on helix C of IL15 were experimentally confirmed to be critical for IL2-Rβ mediated proliferation signals [6].

Sequence analysis revealed that the wild-type IL15 has three putative N-glycosylation sites at Asn71, Asn79 and Asn112. Asn71 is located at the end of helix C [4] and is adjacent to Asn72, whose mutation to other residues affects the IL15-Rβ mediated proliferation of 32Dβ cells [6]. Asn79 is located at the C-D loop, some distance from the binding sites of IL15-Rα, IL-2Rβ and γc [4]. Asn112, however, is located at the end of helix D and is predicted to form a hydrogen bond with the hydroxyl moiety of Tyr103 of γc [5].

Despite the similarity in the tertiary structure of the two proteins, IL15 and IL2 share low sequence homology and play distinct roles in the regulation of the immune response. Although both IL15 and IL2 promote T cell proliferation, IL2 is known to be involved in development

*Abbreviations:* IL15, interleukin 15; IL2, interleukin 2; IL2R, interleukin 2 receptor; IL15R, interleukin 15 receptor; rhIL15, recombinant human interleukin 15; ER, endoplasmic reticulum; ELISA, enzyme-linked immunosorbent assay; $EC_{50}$, half maximal effective concentration; $R_{max}$, maximal response; GAPDH, glyceraldehyde-3-phosphate dehydrogenase

* Corresponding author.
*E-mail address:* huanghaomin@3sbio.com (H. Huang).
[1] These authors contribute equally for this study.
[2] Current address: 3SBio Inc., 399, Libing road, Pudongxin, Shanghai, 201203, China.

https://doi.org/10.1016/j.pep.2018.03.010
Received 1 March 2018; Received in revised form 22 March 2018; Accepted 24 March 2018
Available online 26 March 2018
1046-5928/ 

and suppressive functions of $CD4^+$ $CD25^+$ regulatory T cells (Treg) and mediate activation-induced cell death (AICD) [7]. On the other hand, IL15 enhances $CD8^+$ memory T cell survival [8,9] and is essential for NK cell expansion and development [10]. IL15 generally displays a much better safety profile in animal studies relative to IL2 [11–13]. However, in phase I clinical trials, bolus IV administration of rhIL15 at 1 μg/kg/day demonstrated a dose-limiting toxicity, where 2 of 4 patients had persistent grade 3 alanine aminotransferase and aspartate aminotransferase elevation [14]. These adverse effects were concurrent with the dramatic increase of circulating IL6 and INFγ, indicating that the secondary release of these cytokines may be the cause for the dose-limiting of IL15. Thus, reduction of the Cmax of circulating IL15 below the threshold of triggering secondary cytokine release is important for maintaining a good safety profile. For this reason, a targeted delivery of IL15 to tumors would be a promising strategy for enhancing the therapeutic index of IL15.

Another limitation for IL15 therapeutic use is its size. IL15 is below 15 KDa and thus is expected to be readily filtered by the renal glomerulus [15]. The short pharmacokinetic profile of IL15 has been confirmed in various animal studies [16,17]. Thus, designing a dosing schedule to maintain the therapeutic relevant concentration in the body with low toxicities becomes problematics. It has been shown that serum albumin has a long half-life in circulation due to its size (67 KDa) and recycling by FcRn [18]. Proteins either linked directly to albumin or to an albumin binding domain (ABD), peptides or antibody fragments, have also been shown to have extended serum half-lives [19]. More importantly, proteins binding to albumin appear to accumulate in the solid tumors, probably due to the so-called extended permeability and retention (EPR) effect [20]. These observations provide the justification to make a recombinant IL15 consisting of an albumin binding moiety (ABD) to overcome its short serum half-life and to enhance its tumor targeting ability.

Another barrier towards therapeutic development is that production of IL15 protein by mammalian cells is generally low [21]. Bamford and colleagues showed that IL15 transcription, translation and post-translation are all regulated tightly [22]. The 5′ untranslated region (5′-UTR), an extraordinary long signal peptide (48 amino acid) and the coding sequence for its C-Terminus were all associated with the low expression of the protein. More recently, two independent groups demonstrated that IL15Rα stabilizes IL15 intracellularly by formation of IL15-IL15Rα complexes in the ER or early Golgi [23,24]. Thus, IL15Rα appears to act as chaperones for stabilization of newly synthesized IL15, since IL15 protein cannot be efficiently produced in $IL15R\alpha^{-/-}$ cells, nor from HEK293 cells transfected with IL15, without co-expression of IL15Rα genes [23–25].

Recombinant IL15 has been produced in other ways, but the yields are generally low [21]. Because glycosylation of IL15 is not essential for its bioactivities, expression by E. coli is a popular way to produce recombinant IL15. However, recombinant IL15 expressed from E. coli aggregates into inclusion bodies. Denature and refolding is required to restore biologically active proteins [21,26]. In addition, for recombinant bispecific IL15 proteins with more than one functional moiety, such as IL15 fused with an antibody or antibody fragments, where glycosylation of the non-IL15 domain is not dispensable, *E. coli* system is not an option.

In this study, we demonstrated that we successfully generated a stable HEK293 cell line that can efficiently produce recombinant IL15 fused with an ABD (albumin binding domain) scFv to its C-terminus (IL15-A10m3), by site directed mutagenesis of IL15. These alterations allow for scaled up production up to 50 mg/L and deliver over 10 mg/L of > 95% pure monomeric recombinant fusion proteins after a simple 2 step purifications. The capacity can be scaled up even further by process development. The bioactivity of the initial products in the CTLL2 proliferation assays was lost, at least partly due to the N-glycosylation of IL15. After another round of site-directed mutagenesis, a mutein that can stimulate CTLL2 T cell proliferation comparable to WT IL15 was successfully selected. Using a set of single and double mutations, we further demonstrated that 1) binding of IL15 with IL15 β receptor is a rate limiting step to initiate IL15 signal transduction, since mutants that interfere with IL15-IL15 β receptor interactions dramatically extended $EC_{50}$ in CTLL2 proliferation assays; 2) engagement of IL15 with the γc receptor is required for its full signal transmission.

## 2. Materials and methods

### 2.1. Cell culture

HEK293T was purchased from American Type Culture Collection (ATCC, Manassas, VA). HEK293T were cultured in DMEM medium (Dulbecco's Modified Eagle's Medium) supplemented with 10% heat inactivated fetal bovine serum (HI-FBS), 2 mM L-glutamine and 1% Penicillin/Streptomycin. The murine T cell line, CTLL-2 (ATCC® TIB-214™), was acquired and maintained in a humidified chamber at 37 °C and 5% $CO_2$ in growth medium consisting of RPMI-1640 supplemented with 10% T-STIM with Con-A (Corning), and 10% HI-FBS, 200 mM L-glutamine, 100 mM Sodium Pyruvate, 55 mM 2-mercaptoethanol, 100U/ml Penicillin and 100 μg/ml Streptomycin (Gibco). All cell culture medium and regents were purchased from Thermo Fisher Scientific (Waltham, MA).

### 2.2. RT-PCR and mutagenesis

Human IL-15-A10m3 cDNAs were amplified by reverse transcriptase PCR (Invitrogen) from total RNA obtained from HEK293T cells transiently-transfected pSEC_hIL15-A10m3 using the RNeasy kit (Qiagen). The following primers were used: forward-5′-GGGTGAACGT GATTTCCGACC and reverse-5′-GGACGATGTGCACAAAGGACTG.

Site-directed mutagenesis was used to generate hIL-15-A10m3 muteins. Gene synthesis, mutagenesis and subsequent cloning were all performed by GenScript (Piscataway, NJ).

### 2.3. Gene expression and protein production

To express hIL-15-A10m3 variants (Table 1), the coding sequences were inserted between AscI and XhoI cloning sites in the mammalian expression vector pSecTag2 A (Invitrogen). $(G4S)_5$ was used as a linker between the albumin binding domain A10m3 and the hIL-15 or hIL-15 mutein. In the case of the single-chain IL15Rα (sushi) construct, an 85 AA sequence including the IL15Rα (sushi) domain as well as the original linker [27] was fused to the N-terminus of IL15 domain. The resulting expression vectors were transfected into HEK293T cells using 1 μg/ml PEI, followed by selection in medium containing 250 μg/ml Zeocin (Invitrogen) for 2–3 weeks. Preliminary clones stably transfected with the expression vectors were picked and sub-cultured in the 24 well plates. The medium from the sub-cultured clones were tested for

**Table 1**
A list of $IL15_{K86R}$-A10m3 muteins were made for this study and the corresponding interaction receptors respectively.

| Muteins | related receptors |
|---|---|
| $IL15_{k86R}$-A10m3-N112Q | γc |
| $IL15_{k86R}$-A10m3-N112S | γc |
| $IL15_{k86R}$-A10m3-N112A | γc |
| $IL15_{k86R}$-A10m3-N71A | IL15/IL2 Rβ |
| $IL15_{k86R}$-A10m3-N79A | N/A |
| $IL15_{k86R}$-A10m3-N72D | IL15/IL2 Rβ |
| $IL15_{k86R}$-A10m3-N112Q-N71A | γc, IL15/IL2 Rβ |
| $IL15_{k86R}$-A10m3-N112Q-N79A | γc |
| $IL15_{k86R}$-A10m3-N112A-N79A | γc |
| $IL15_{k86R}$-A10m3-N112A-N79D | γc |
| $IL15_{k86R}$-A10m3-N112A-N71D | γc, IL15/IL2 Rβ |
| $IL15_{k86R}$-A10m3-N112A-N72D | γc, IL15/IL2 Rβ |

recombinant protein productivity and bioactivity. Resulting clones with the highest protein expression level and activity were further expanded for protein production. For protein production, $1 \times 10^8$ cells were seeded in 550 ml complete medium for each ten-layer hyperflask (Cat#09-761-22, Corning). After reaching confluence (2–3 days), the medium was replaced with production medium that was supplemented with 0.5% FBS for 10 days.

His tag recombinant proteins present in cell culture supernatants were purified using an Akta Avant 25 protein purification system. The filtered supernatant was loaded into a Histrap HP 5 ml column (GE healthcare cat# 17-5248-01) equilibrated in 1X phosphate buffered saline +150 mM NaCl, 5 mM imidazole pH 7.5 at a flow rate of 2.5 mL/min. The column was washed with ten column volumes of 1x phosphate buffered saline +150 mM NaCl, 30 mM imidazole pH 7.5. Protein was eluted from the column using 1X phosphate buffered saline +150 mM NaCl, 300 mM imidazole pH 7.5 and collected in 1 mL fractions. Fractions containing protein of interest was determined by performing size exclusion UPLC on the elution fractions. IMAC purified protein fractions were loaded onto a Hiload 16/600 Superdex 200 pg gel filtration column that was equilibrated with 50 mM Tris-Cl pH7.5, 300 mM NaCl, 0.02% Tween 80. Chromatography flow rate was at 0.45 mL/min. Protein eluate was collected in 1 mL fractions. Protein of interest was determined by performing size exclusion UPLC on the elution fractions. Fractions containing over 95% monomeric proteins were pooled and formulated by adding 100 mM Trehalose.

### 2.4. ELISA

96-well microtiter plates were coated with 10 μg/ml mouse serum albumin (Cat# MSA62, Equitech Bio) or 1 μg/ml recombinant human IL-15 alpha receptor Fc chimera protein (Cat#7194-IR-050, R&D System) in 1x phosphate buffered saline buffer (PBS, PH 7.0) for overnight at 4 °C. The plates were washed thoroughly, blocked with SuperBlock™ blocking buffer (Cat#37516, Thermo Fisher) and incubated with culture supernatants from HEK293T cells expressing recombinant hIL-15-A10m3 or hIL-15-A10m3 muteins for 1 h at room temperature. The plates were washed and incubated with 0.5 μg/ml of HRP conjugated anti-His monoclonal antibody H8, (MA121315HRP, Invitrogen) for 1 h at room temperature. The plates were washed and the reaction developed with addition of TMB Substrates (Cat#34028, Pierce) for 2–3 min. The reaction was stopped by adding 2 M $H_2SO_4$ and the plates were read with a Synergy H1 hybrid Multi-Mode Reader (BioTek Instruments, Inc.) at 450 nm.

### 2.5. Deglycosylation & glycan staining

The deglycosylation of hIL-15-A10m3 proteins and muteins was performed under native condition by using Promega™ protein deglycosylation kit (Cat# V4931, Promega). Briefly, 2 μl of 10X reaction buffer, 2 μg glycoprotein, 2 μl of deglycosylation mix and water were added to the tube to give a final reaction volume of 20 μl. In the control group, deglycosylation mix with the same volume of water was made to give a final reaction volume of 20 μl. Both the experiment group and control group were incubated in the 37 °C water bath for 4 h, and then the products were analyzed using SDS-PAGE with Glycan staining. The Glycan staining was performed by using pierce glycoprotein staining kit (Cat# 24562, Thermo Scientific), following the manufacturer's introduction.

### 2.6. CTLL-2 cell proliferation assay

Prior to use, the CTLL-2 cells were harvested in logarithmic phase and washed 3 times in RPMI-1640 without supplements. Cells were resuspended in assay medium (RPMI-1640 supplemented with 10% hi-FBS only) at $5 \times 10^5$ cells/ml and placed at rest for 4 h in a humidified chamber at 37 °C and 5% $CO_2$. After 4 h, varying dilutions of recombinant human IL-15 (R&D Systems) and test IL-15 samples were prepared in 100 μL assay medium in the wells of a 96-well cell culture cluster plate. Rested CTLL-2 cells were added to each well at $5 \times 10^4$ cells/well for a final reaction volume of 200 μL, and the plates incubated for 48 h at 37 °C and 5% $CO_2$. After 44 h, 40 μL MTS reagent (CellTiter 96® $AQ_{ueous}$ Non-Radioactive Cell Proliferation Assay, Promega) was added as per manufacturer's instructions, and the plates further incubated for 4 h. Finally, the plates were mixed on a vortex mixer (Eppendorf™) with a microwell plate adapter and the plates read at 490 nm on a Synergy H1 hybrid Multi-Mode Reader (BioTek Instruments, Inc.) The biological activities of our purified IL-15 compounds were compared to a commercial recombinant IL-15 standard, and the $EC_{50}$ values determined using GraphPad Prism Software.

### 2.7. SDS PAGE and western blotting

Protein fraction aliquots were diluted in 4X LDS sample buffer +2% SDS. Samples were heated at 90 °C for 3 min, then cooled to room temperature. Reduced samples were electrophoresed through a 10 to 15 well 1.0 mm 4–15% Bis Tris SDS PAGE gel (Thermo Fisher cat# NP0323BOX) at 150 V. After electrophoresis, the gel was stained with Coomassie Brilliant Blue R250 and destained with 40% methanol, 10% acetic acid. Western blot transfer was performed using the ThermoFisher Scientific iBlot blotting system (Thermo Fisher Scientific cat# IB401002). Following transfer of the separated proteins onto the PVDF membrane, the membrane was washed for 5 min with $DIH_2O$, and then 20 mL of Superblock T20 was added to the membrane. Membrane was incubated in the blocking solution for an hour with gentle agitation. After removing from the blocking solution, the membrane was incubated in 10 mL of 1:1000 diluted HRP conjugated anti-hIL15 antibody for 1 h at room temperature. The membrane was washed 3 times with 1X PBS, 0.05% Tween 20 pH 7.5. 10 mL of TMB blotting solution was added and incubated with gentle agitation until proper band development is achieved.

## 3. Results

### 3.1. Expression of IL15-A10m3 protein is limited post-transcriptionally

IL15-A10m3, where the A10m3 is an anti-albumin (both MSA and MSA) scFv (unpublished study), was transfected into HEK293T cells and the culture medium was assayed for secreted protein. However, IL15-A10m3 could not be detected from 3 independent transfections by ELISA (Fig. 1A). By contrast, another interleukin fusion protein with a similar structure format to IL15-A10m3, but significantly larger in size was expressed from transfected cells. This control protein was detected in three-day culture media of transfected cells by both Western blotting and functional ELISA binding to MSA (data not shown).

We next used RT-PCR to monitor expression of IL15-A10m3 mRNA from transfected cells. Results from 4 independent transfections showed increased IL15-A10m3 expression relative to the untransfected control (Fig. 1B). Taken together, these results show that IL15-A10m3 is transcribed in the transfected cells and the failure to detect IL15-A10m3 proteins most likely occurs at the post-transcriptional level.

### 3.2. Identification of a putative ubiquitination site in IL15 that is adjacent to the IL15 receptor alpha binding site

Previous studies have shown that IL15 protein has a short half-life. However, co-expression of IL15Rα with IL15 in the same cell greatly increased the amount of cell surface IL15Rα as well as IL15 [23]. Further evidences confirmed that IL15Rα acts as a chaperone to protect and stabilize IL15 before secretion [25]. These findings suggest that instability of IL15 can be overcome by IL15Rα but how this occurs is unclear. Ubiquitination is commonly used by cells to mark proteins for degradation [28]. Given that IL15 is a very potent proinflammatory

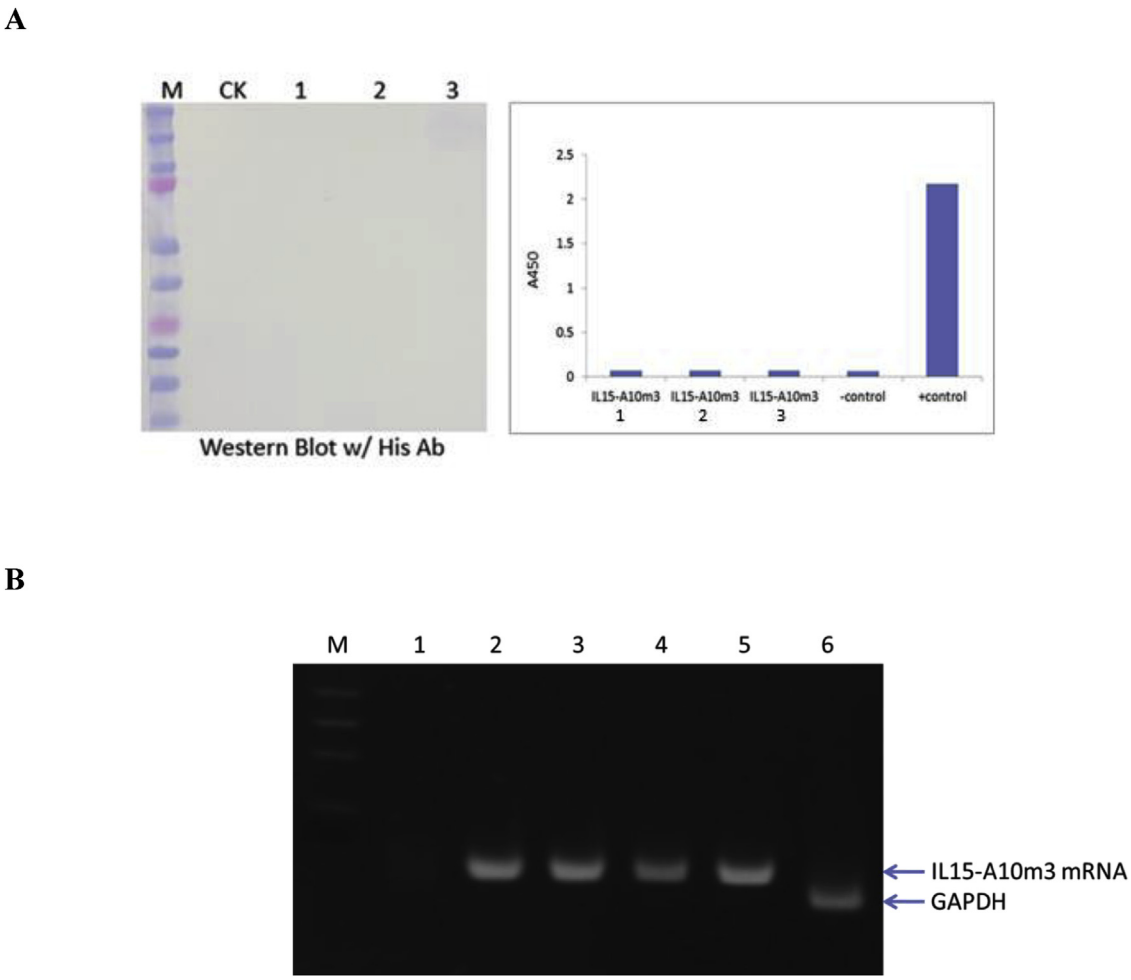


**Fig. 1. Verification of IL15-A10m3 mRNA in transfected cells. A**) Expression of IL15-A10m3 from HEK293 cannot be detected by Western blotting using either anti-His tag antibody (left), or by functional ELISA binding to MSA (right). M: Marker, CK: non-transfected culture medium as control, 1–3: media from 3 independently transfected cell cultures (sample 1, 2 and 3 respectively). 10 μg/ml *E. coli* produced IL15-A10m3 was served as the positive control. **B**) mRNA was prepared from 4 independently IL15-A10m3 transfected cells and RT-PCR was performed to evaluate the mRNA level of IL15-A10m3 in comparison with that of a house-keeping gene, GAPDH. M) Molecular weight ladder; Lane1) untransfected cell control; 2–5) IL15-A10m3 mRNA from 4 transfected cells; 6) GAPDH mRNA positive control.

cytokine, whose expression is tightly controlled by cells, it is possible that cells utilize ubiquitination to actively control IL15 protein levels. Indeed, inspection of the IL15 (www.ubpred.org) identified K86 as a putative ubiquitination site (Fig. 2B). Intriguingly, K86 is adjacent to the IL15Rα binding site (Fig. 2A), bringing up the possibility that the binding of IL15Rα to IL15 blocks the accessibility of an ubiquitin ligase (e.g. E3) to K86.

### *3.3. Mutation of K86 in IL15 restored the expression of the IL15-A10m3 protein by HEK293T cells*

To confirm our hypothesis, the following 3 constructs were made (Fig. 3). A) the sushi domain of IL15Rα fused IL15-A10m3, which should show improved expression as described by other studies [16]; B) a K86A mutation of IL15-A10m3, and C) a K86R mutation of IL15-A10m3. All 3 constructs were transfected into HEK293T cells and stable clonal cell lines were established. Clones for each construct were randomly selected and the culture media from these clones were tested for expression of their respective recombinant proteins.

Expression levels of functional full-length proteins were accessed and compared by functional ELISA, where the signal strengths of the albumin binding domains (A10m3) in all constructs binding to mouse serum albumin (MSA) were measured. In line with our previous finding, 9 out of 12 clones transfected with WT IL15-A10m3 did not express detectable levels of proteins when compared to the negative control. The 3 positive clones expressed < 30% of level seen with the positive control (Fig. 4A). Consistent with other's studies, all IL15Rα-fused IL15-A10m3 clones expressed protein amounts that varied between 20 and 200% seen for the positive control. Importantly, IL15-A10m3 harboring either K86R (6 clones) or K86A (6 clones) mutations were expressed at levels comparable to that of IL15Rα-fused IL15-A10m3 which showed improved expression in ours and other's studies. 7 out of the 12 clones from both K86R and K86A mutants expressed higher amounts of protein than the positive control. Using purified IL15-A10m3 protein for comparison, we estimate that some of the K86A and K86R mutants accumulated to > 20μg/ml in the culture medium. Two of the best producers were K86 mutant clones, A3 and R6. In addition, similar expression profile was also seen for IL15 K86R muteins (Fig. S1).

To demonstrate that K86R and K86A mutations did not impair binding to IL15Rα, these variants were tested for binding to IL15Rα by ELISA. Media from clones R6 and A3 showed strong binding activities to IL15Rα ($A_{450}$ = 1.5) relative to the negative control. Thus, the K86R and K86A mutations did not impair the in vitro binding of IL15-A10m3 to IL15Rα (Fig. 4B). Interestingly, IL15Rα-IL15-A10m3 fusion failed to show any binding to IL15Rα, suggesting that the intramolecular interaction between the IL15Rα sushi domain with IL15 prevented its

**A**

```
1- NWVNVISDLKKIEDLIQSMHIDATLYTESDVHPSCKVT
39-AMKCFLLELQVISLESGDASIHDTVENLIILANNSLSS
77-NGNVTESGCKECEELEEKNIKEFLQSFVHIVQMFINTS
```

**B**

**Output:**

| Residue | Score | Ubiquitinated |
|---|---|---|
| 10 | 0.41 | No |
| 11 | 0.43 | No |
| 36 | 0.43 | No |
| 41 | 0.36 | No |
| 86 | 0.68 | Yes Low confidence |
| 94 | 0.53 | No |
| 97 | 0.51 | No |

**Legend:**

| Label | Score range | Sensitivity | Specificity |
|---|---|---|---|
| Low confidence | 0.62 ≤ s ≤ 0.69 | 0.464 | 0.903 |
| Medium confidence | 0.69 ≤ s ≤ 0.84 | 0.346 | 0.950 |
| High confidence | 0.84 ≤ s ≤ 1.00 | 0.197 | 0.989 |

**Fig. 2. Identification of the potential ubiquitination site in IL15 sequence.** **A**) K86 in red is a putative ubiquitination site which is next to the IL15Rα binding sites (marked by stars); **B**) K86 is a hit for ubiquitination from UbPred, an online ubiquitination site database (www.ubpred.org). (For interpretation of the references to colour in this figure legend, the reader is referred to the Web version of this article.)

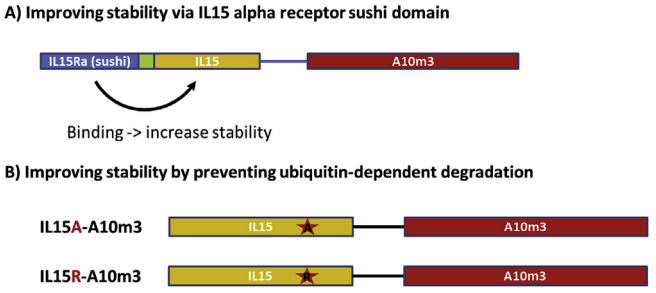


**Fig. 3. Schematic of the putative ubiquitination resistant constructs.** **A**) single-chain IL15Rα-IL15-A10m3 construct used as a positive control; **B**) K86A and K86R mutation constructs.

binding to an external source of IL15Rα (Fig. 4B).

To evaluate the productivity of the K86 mutant, we chose the strongest producing clone R6 of $IL15_{K86R}$ -A10m3 for scaled-up production. Medium was harvested after 10 days' growth and the recombinant protein was purified by affinity IMAC chromatography, followed by size-exclusion chromatography (SEC). The protein amounts from the IMAC column was 30 mg/L. Given the efficiency of the IMAC chromatography is approximately 60%, the total proteins in the medium is about 50 mg/L. SEC chromatograms showed 41% of the total product is monomer (Fig. 5A), which contrasts with the 5% monomer for re-folded IL15-A10m3 expressed in *E. coli* (data not shown). Furthermore, SDS-PAGE and Western blotting confirmed that 10 mg/L of the final product with a monomer purity > 95% was obtained from this production run (Fig. 5B and C).

Finally, we used Octet to measure the binding activity of the purified $IL15_{K86R}$-A10m3 to mouse serum albumin (MSA). The results show the equilibrium dissociation constant (KD) of 28.9 nM, in line with that of IL15-A10m3 produced from *E. coli* (Fig. 5D).

### *3.4. The bioactivity of $IL15_{K86R}$-A10m3 produced from HEK293T cells requires de-glycosylation*

It has been demonstrated that N-terminal IL15 fusion proteins have impaired bioactivity to stimulate CTLL2 cell proliferation [29]. Thus, we tested our proteins using CTLL2 proliferation assays. Consistent with other's findings, HEK293 produced $IL15_{K86R}$-A10m3 proteins from 3 different batches lost 75% of their ability to simulate CTLL2 growth ($R_{max}$), when compared to that of WT IL15 (R&D) and our in-house produced IL15-A10m3 proteins from *E. coli* (Fig. 6A) in MTS assays. The specific activity ($R_{max}$/pM) for proliferation of CTLL2 cells stimulated by both WT IL15 (R&D) and IL15-A10m3 from *E. coli* is 0.025, while all 3 batches of $IL15_{K86R}$-A10m3 showed specific activities of $6.25 \times 10^{-4}$, approximately 40-fold lower. To understand the differences in activities, we tested the idea might be due to differences in glycosylation which is lacking from the E. coli produced protein. Thus, we hypothesized that glycosylated $IL15_{K86R}$-A10m3 produced from mammalian cells may reduce its activity. To confirm this hypothesis, we de-glycosylated $IL15_{K86R}$-A10m3 with PNGase enzyme mix. SDS-PAGE showed PNGase treatment shifted migration to a sharper band migrating at 43KD which is close to the calculated molecular weight. This contrasts with untreated samples which displayed an observed molecular weight over 50 KDa (Fig. 6B right). This suggests that PNGase treatment removed glycans ligated on the protein. Indeed, glycan staining further confirmed the observation, as samples treated with PNGase were not visible, while the untreated samples showed clear pink bands (Fig. 6B left), which show that the protein produced by mammalian cells is indeed glycosylated.

Next, CTLL2 proliferation assay was carried out using the deglycosylated $IL15_{K86R}$-A10m3 (Fig. 6C). Control samples, either no treatment or mock treated $IL15_{K86R}$-A10m3 showed low activity (25% of the control $R_{max}$) as seen previously. In contrast, the deglycosylated $IL15_{K86R}$-A10m3 strongly stimulated CTLL2 proliferation (> 90% of the control $R_{max}$), indicating that $IL15_{K86R}$-A10m3 bioactivity is indeed impaired by glycosylation.

### *3.5. N112 of $IL15_{K86R}$-A10m3 is critical for its full bioactivity ($R_{max}$) to promote CTLL2 proliferation*

We next began to investigate the effects of glycosylation of $IL15_{K86R}$-A10m3 on bioactivity. There are 3 putative glycosylation sites, N71, N79 and N112 on IL15 [4]. We first attempted to produce a triple mutant, where all three putative glycosylation sites were mutated to mimic non-glycosylated $IL15_{K86R}$-A10m3 from HEK293T cells. However, the expression of this mutant was so low that it could not be effectively purified (data not shown).

To understand the glycosylation patterns of $IL15_{K86R}$-A10m3, a series of muteins of glycosylation sites of the IL15 domain were made using site-directed mutagenesis (Table 1). Both SDS-PAGE and glycan staining were used to assess the extent of glycosylation before and after PNGase treatment. $IL15_{K86R}$-A10m3 N112Q and $IL15_{K86R}$-A10m3 N112A muteins migrated slightly faster than that of parental $IL15_{K86R}$-A10m3 on SDS-PAGE, suggesting that N112 is a glycosylation site (Fig S2 A, B). A double mutation, $IL15_{K86R}$-A10m3 N112Q + N79A, migrated even faster than N112Q and N112A single mutants did, but still slightly slower than PNGase treated samples. Thus, N71 is most likely glycosylated besides N79 and N112 (Fig S2 A, B). $IL15_{K86R}$-A10m3 N112A + N71D double mutant migrated to the same position as $IL15_{K86R}$-A10m3 N112Q + N79D did in SDS-PAGE, suggesting that N79 is also likely glycosylated (Fig S2 C). Indeed, glycan staining demonstrated the existence of glycan on all parental, single and double mutants with a gradually diminished intensity that corresponded with their migration in SDS PAGE (Fig S2 B, C). Deglycosylation of all proteins by PNGase was complete since the different proteins migrated to the same position as did E. coli produced IL15-A10m3 (Fig S2 A). Taken together, all 3 glycosylation sites of the IL15 domain appears to be

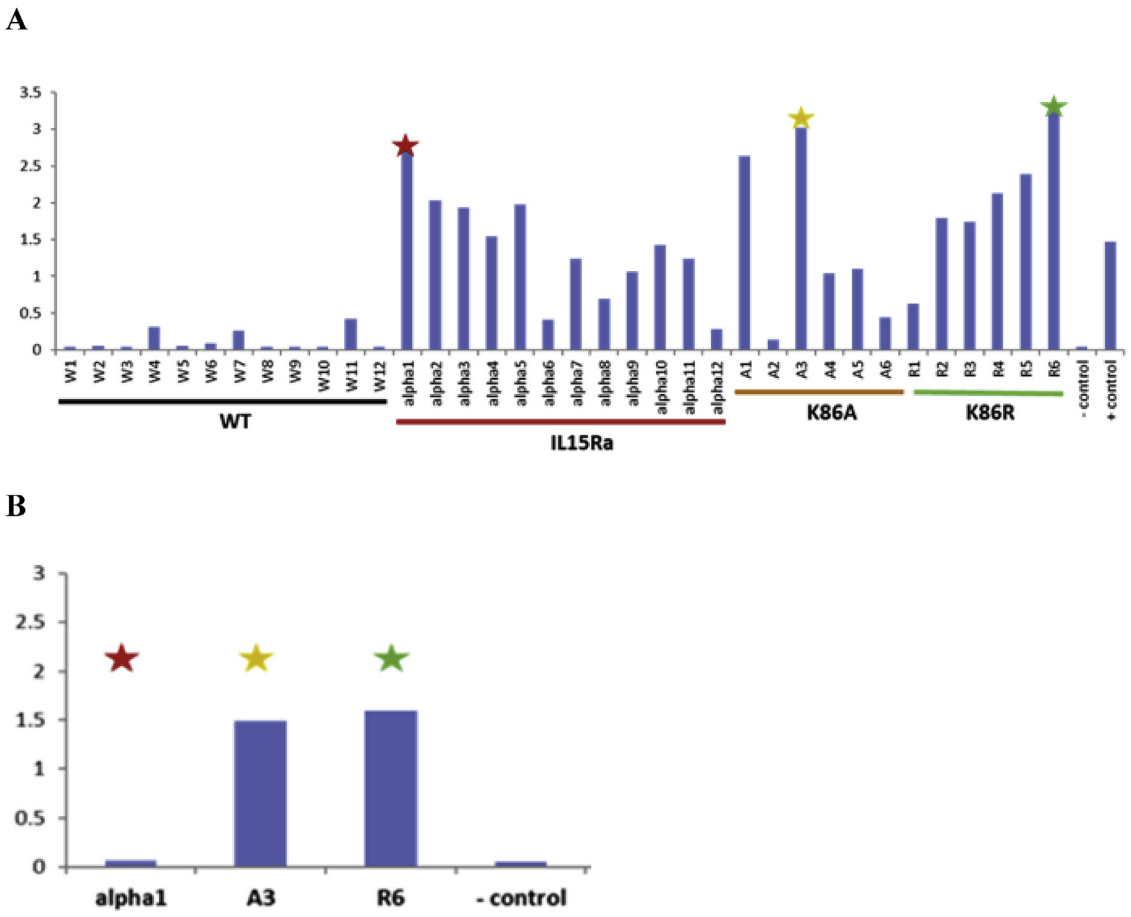


**Fig. 4. Mutation of K86 in IL15 domain restored the expression of IL15-A10m3 from HEK293T cells to the level comparable to IL15Rα-IL15-A10m3. A)** 12 individual clones of IL15-A10m3 (WT), 12 individual clones of IL15Rα-IL15-A10m3 (IL15Ra), 6 individual clones of $IL15_{K86A}$-A10m3 (K86A) and 6 individual clones of $IL15_{K86R}$-A10m3 (K86R) transfected cells were brought up to confluence. The culture medium of each clone was collected and tested for the concentrations of functional full-length proteins by measuring the binding of A10m3 (ABD) to MSA in ELISA. Non-transfected culture medium was used as the negative control. 10 μg/ml *E. coli* produced IL15-A10m3 was served as the positive control. Stars denote the highest producers: alpha1 of IL15Ra clones (red), A3 of K86A clones (yellow) and R6 of K86R clones (green). **B)** The best producing clone of each group, alpha1 (red star), A3 (yellow star) and R6 (green star) was verified for their ability to bind to IL15Rα in a functional ELISA, where 1 μg/ml IL15 receptor α was coated on a 96 well plate. Non-transfected culture medium was used as negative control. (For interpretation of the references to colour in this figure legend, the reader is referred to the Web version of this article.)

glycosylated in our study.

Surprisingly, the single N112A mutant successfully rescued the bioactivity of $IL15_{K86R}$-A10m3 to stimulate CTLL2 proliferation to the level comparable to recombinant human IL15 (rhIL15), while the productivity was not impaired when compared to the parental $IL15_{K86R}$-A10m3 (Fig. 7A and S3). More importantly, $IL15_{K86R}$-A10m3 N112A also showed full capabilities in stimulating T and NK cell expansions as well as prolonging PK relative to WT hIL15 in vivo (unpublished data). These results suggest that a glycosylation-like bulky structure at residue 112 may undermine the bioactivity of $IL15_{K86R}$-A10m3. It is worth noting that the initial mutein, N112Q, failed to show any improvement in bioactivity compared to the parental $IL15_{K86R}$-A10m3 (Fig. 7B). One possibility is that Q112 cannot form the hydrogen bond to Tyr103 of γc like N112 [5]. Since S130 of IL2 is also predicted to form a hydrogen bond to Tyr103 of γc, a N112S mutein was made and tested. Interestingly, $IL15_{K86R}$-A10m3 N112S indeed showed improved bioactivity ($OD_{490}$ of $R_{max}$ = 0.8) relative to N112Q mutein ($OD_{490}$ of $R_{max}$ = 0.6), but cannot rescue the activity to the $R_{max}$ level of $IL15_{K86R}$-A10m3 N112A ($OD_{490}$ of $R_{max}$ = 1). It was intriguing to see that the recovered bioactivities, in terms of $R_{max}$, are inversely proportional to the size of the side chain (Q > S > A) of the residue 112 (Fig. 7B), suggesting that the residue 112 may interrupt the interaction of IL15 with the γc receptor following the size increase and thus undermine signal transduction.

Nevertheless, we successfully established a stable cell line of $IL15_{K86R}$-A10m3 N112A, which can readily produce milligram quantities of fully active recombinant proteins using adherent HEK293T cells in tissue culture flasks.

### *3.6. N71 of $IL15_{K86R}$-A10m3 is important for initiation of IL15-induced CTLL2 proliferation*

Unlike residue 112 whose changes significantly affected the $R_{max}$, residue 71 appeared to affect the $EC_{50}$ in T cell proliferation assays. When comparing $IL15_{K86R}$-A10m3 N112Q with $IL15_{K86R}$-A10m3 N71A and $IL15_{K86R}$-A10m3 N112Q + N71A in CTLL2 T cell proliferation assays, the former has a $EC_{50}$ of 10.22pM, about 12.5-fold lower than that of the latter two, 134pM and 127.9pM respectively (Fig 8). The significant increase of concentration for N71A mutants to stimulate CTLL2 proliferation suggests that residue 71 is critical for initiation of IL15-induced CTLL2 T cell proliferation, probably via interaction with IL15β receptor [6]. Changing from Asparagine to Alanine at this position somehow impaired this interaction.

## 4. Discussion

In this paper, we have systematically assessed the intrinsic characteristics of IL15-scFv fusion protein and have devised a novel strategy

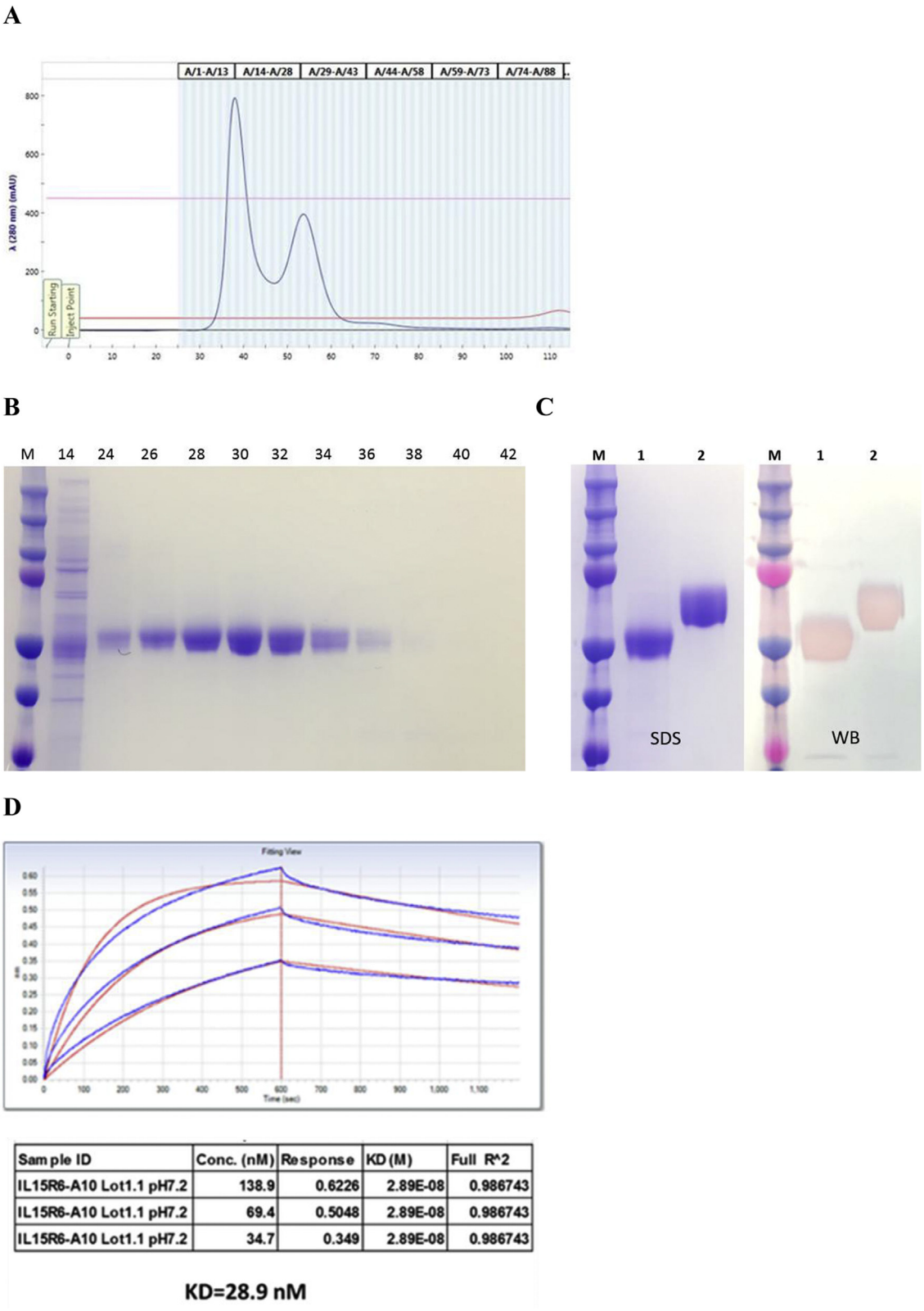


| Sample ID | Conc. (nM) | Response | KD (M) | Full R^2 |
|---|---|---|---|---|
| IL15R6-A10 Lot1.1 pH7.2 | 138.9 | 0.6226 | 2.89E-08 | 0.986743 |
| IL15R6-A10 Lot1.1 pH7.2 | 69.4 | 0.5048 | 2.89E-08 | 0.986743 |
| IL15R6-A10 Lot1.1 pH7.2 | 34.7 | 0.349 | 2.89E-08 | 0.986743 |

**Fig. 5. Scale-up production of IL15$_{K86R}$-A10m3 clone #6. A**) Chromatograph of IL15$_{K86R}$-A10m3 by a Size exclusion column; **B**) SDS-PAGE analysis of the SEC fractions from 14 to 42; **C**) Final products **1:** IL15$_{K86R}$-A10m3, **2:** IL15Rα-IL15-A10m3 were confirmed by SDS-PAGE (left) and Western blotting with anti-His tag antibody (right). **D**) Octet shows the KD of IL15$_{K86R}$-A10m3 binding to MSA is 28.9 nM, in line with that of proteins produced from *E. coli*.

that readily produces milligram quantities of an IL-15 fusion protein, IL15$_{K86R}$-A10m3 N112A, using HEK293T cells. Recombinant IL15 expression from mammalian cells has been proven to be very difficult. Mallinder, PR and his colleagues tried different ways to optimize IL15 expression from mammalian expression systems, using MEL cells or HEK-EBNA cells as well as a number of different leader sequences, but were unable to detect any soluble IL15 in the supernatants of those cells by Western blot [21]. Consistent with their experiences, we also failed

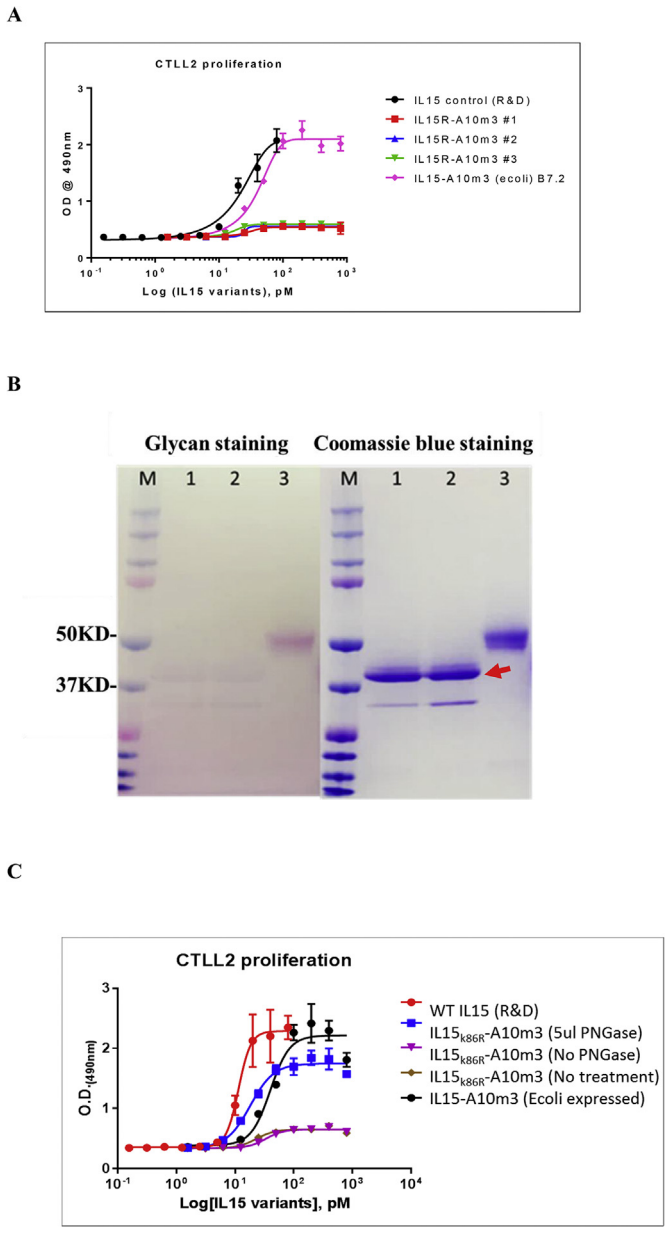


**Fig. 6. Deglycosylation of IL15$_{K86R}$-A10m3 using PNGase enzyme mix restored the bioactivity in CTLL2 proliferation assays. A**) CTLL2 proliferation assays showed IL15$_{K86R}$-A10m3 produced from HEK293T has reduced bioactivity. Three different samples of IL15$_{K86R}$-A10m3 (IL15R-A10m3 batch #1-#3) produced from HEK293T showed a significantly reduced activity to promote CTLL2 proliferation in comparison to commercial WT IL15 (R&D), which is produced from E. coli and in-house E. coli produced IL15-A10m3 (B7.2). **B**) After PNGase enzyme mix treatment under native conditions, N-Glycan was completely removed and visualized by Glycan staining (left) and coomassie blue staining (right) following SDS-PAGE. Lane1: IL15$_{K86R}$-A10m3 + 5μl PNGase mix; 2: IL15$_{K86R}$-A10m3 + 10μl PNGase mix; 3: Mock treatment (no enzyme) control. Red arrow denotes the deglycosylated IL15$_{K86R}$-A10m3. The small bands (< 37KD) in the treated sample lanes are one of proteins from the enzyme mix. **C**) Deglycosylated IL15$_{K86R}$-A10m3 (Blue) showed recovered activity in CTLL2 proliferation assays, in comparison with Mock-treated and no-treatment samples (purple, dark yellow). WT IL15 from R&D systems (red) and in-house E. coli produced WT IL15 (Black) was used as the positive control. (For interpretation of the references to colour in this figure legend, the reader is referred to the Web version of this article.)

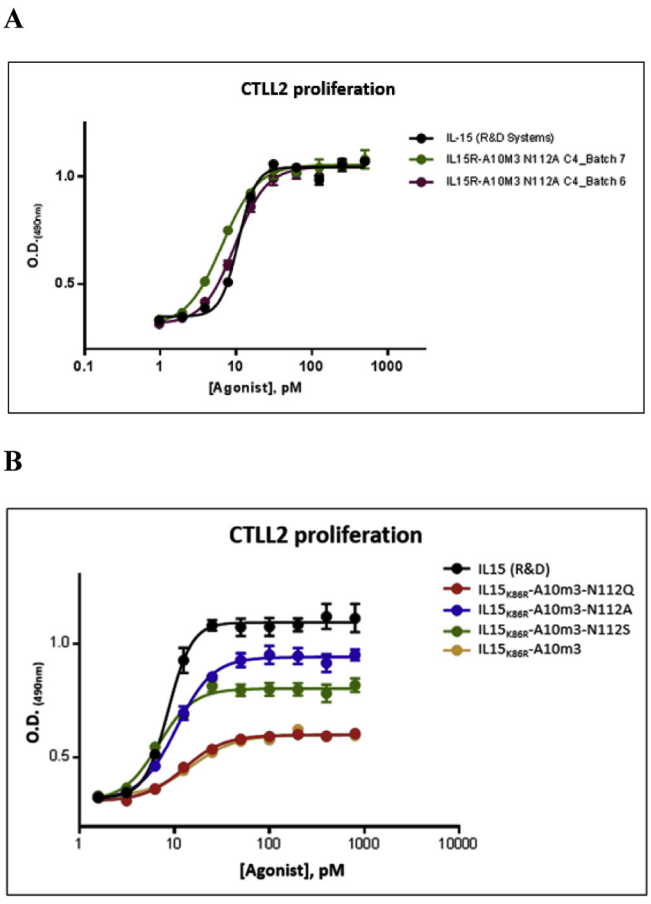


**Fig. 7. N112A mutation of IL15$_{K86R}$-A10m3 restored its bioactivity comparable to that of recombinant human IL15 in CTLL2 proliferation assays. A**) two batches of N112A mutation (green) and (purple) of IL15$_{K86R}$-A10m3 produced from a clonal cell line C4 restored the CTLL2 proliferation activity comparable to recombinant human IL15 (black) from R&D systems. **B**) mutations with different side chains at N112 were tested to demonstrate the size effect on the bioactivity. N112Q (big, red), N112S (medium, green) and N112A (small, blue) displayed bioactivities inversely proportional to the size of the side chains. WT IL15 from R&D systems (black) was used as the positive control. Parental IL15$_{K86R}$-A10m3 (yellow) was used as the negative control. (For interpretation of the references to colour in this figure legend, the reader is referred to the Web version of this article.)

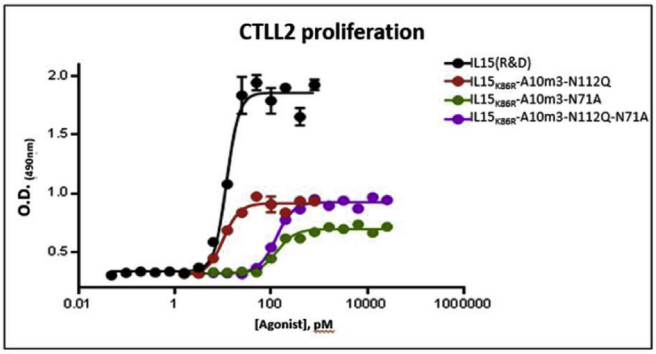


**Fig. 8. Mutation of N71 to A71 of IL15$_{K86R}$-A10m3 variants significantly increased the EC$_{50}$ in CTLL2 proliferation assays.** Recombinant human IL15 from R&D systems is the positive control (black). EC$_{50}$ of IL15$_{K86R}$-A10m3-N112Q (red), IL15$_{K86R}$-A10m3-N71A (green) and IL15$_{K86R}$-A10m3-N112Q-N71A (purple) were compared in CTLL2 proliferation assays. (For interpretation of the references to colour in this figure legend, the reader is referred to the Web version of this article.)

to detect soluble WT IL15-A10m3 in the supernatants of HEK293T cells by either Western blot or by SDS-PAGE in our initial attempts. Subsequent analysis using RT-PCR, however, demonstrated that mRNAs of WT IL15-A10m3 was transcribed in transfected cells. It was shown that IL15 proteins have a short half-life in cells and require co-expression of IL15 receptor α to stabilize them before secretion [23,25], suggesting that post translational modification may play a role in this process. Ubiquitination is commonly used by cells to remove unwanted proteins. Indeed, inspection of IL15 sequence allowed us to identify K86 as a putative ubiquitination site. Given that K86 is adjacent to the IL15Rα binding sites, it is plausible that IL15Rα binding can prevent IL15 from being ubiquitinated and degraded. Indeed, 7 out of 12 K86A and K86R mutants expressed more proteins than the positive control, which is on par with the IL15Rα-fused IL15-A10m3 clones. By contrast, there were no detectable amounts of recombinant proteins from 9 out of 12 WT IL15-A10m3 clones. Scale-up production of the highest producer of K86R mutants, $IL15_{k86R}$-A10m3, successfully accumulated up to 50 mg/L proteins in the culture medium, and was able to deliver up to 10 mg/L of > 95% pure monomeric recombinant fusion proteins after 2-step purification from the medium. It is worth noting that adherent HEK293T cells were used for the above productions, which have some drawbacks when compared to suspension CHO K1 cell derivatives, such as difficulties in scaling up due to space limitations, difficulties in reaching high cell densities, as well as lacking gene amplification capabilities etc. It is most likely that the yield of $IL15_{k86R}$-A10m3 can be further boosted by process development using suspension CHO derivatives.

Unlike *E. coli*, $IL15_{k86R}$-A10m3 expressed from HEK293T cells is glycosylated. Inspection of IL15 sequence revealed 3 putative glycosylation sites, N71, N72 and N112. We found all 3 sites of $IL15_{k86R}$-A10m3 from HEK293T cells were glycosylated, using SDS-PAGE and glycan staining following PNGase treatment. Interestingly, a recent study demonstrated that the N79 of the recombinant IL15 derived from HEK293 cells is the only N-glycosylated site detected by LC-MS/MS, while the other two potential sites (N71 and N112) were unoccupied [30]. The discrepancy between the two findings is not clear, however, the differences in cell lines, growth conditions as well as the protein structures cannot be ruled out. Nevertheless, HEK293 expressed $IL15_{k86R}$-A10m3 lost 75% of its bioactivity in stimulating CTLL2 T cell proliferation, while deglycosylation by PNGase significantly improved the activity, suggesting that glycosylation played a role in this event. When working with the IL15-L19 fusion protein, the Neri group also showed that the protein was glycosylated and treatment with PNGase was able to improve its ability to stimulate CTLL2 proliferation [29]. Our observation is consistent with Neri's finding.

Initially, we tried to improve the activity of $IL15_{k86R}$-A10m3 by mutating all 3 N-glycosylation sites, but this failed because the mutant was poorly expressed. This result suggests that glycosylation of IL15 may be required for its expression from HEK293 cells. However, mutation of one or two of the 3 putative N-glycosylation sites did not significantly impair the expression. Critically, a single mutant, $IL15_{k86R}$-A10m3 N112A, showed full activity when compared to WT hIL15, suggesting that residue 112 is the key site that affects bioactivities of IL15 domain through interaction with γc receptor. It was suggested that a hydrogen bond is formed in between N112 of IL15 and Y103 of γc receptor [5]. However, our data suggest such a bond is not critical for IL15 signaling through γc receptor. Furthermore, the size of the side chain (Q > S > A) of residue 112 is inversely proportional to the $R_{max}$ of IL15 activities, suggesting that the side chain of residue 112 may interfere with the interaction of IL15 with γc receptor following its size increase. Next, we then showed that HEK293T produced $IL15_{K86R}$ was fully capable of stimulating T cell proliferation without the need of N112A mutation (Fig S4). This observation suggests that the bulky effect at residue 112 occurs only when the C-terminus of IL15 is fused to an extra domain. The loss of activity seen with glycosylation and the size of residue 112 is specific to IL15 fusion proteins. Nevertheless, our research demonstrated that the residue 112 of IL15 domain is indeed critical for establishing the signal transduction between $IL15_{k86R}$-A10m3 and γc receptor and that signaling through γc receptor is required for cells to reach the maximum response ($R_{max}$).

In addition, we found that replacement of Asparagine to Alanine at residue 71 increased $EC_{50}$ of $IL15_{k86R}$-A10m3 up to 12.5-fold in T cell proliferation assays. Intriguingly, substitution of N72 (Asparagine) to Aspartic acid (D) or Alanine (A), an adjacent site to N71, was reported to provide a 4–5-fold increase in bioactivity, in terms of $EC_{50}$, of a CHO-derived recombinant IL15 variant using 32Dβ cell proliferation assays [6]. Since the bioactivity increase can only be observed in 32Dβ cell model (IL2β/γc complex), but not in CTLL2 (IL15α/β/γc complex) model, the enhanced activity was attributed to the improved interaction between IL15β receptor and the helix C of IL15, a ligand: receptor contact interface identified by the crystal structure [5]. Most likely, N71 of IL15 is also involved in IL15 mediated IL2β receptor signal transduction, and this interaction is a rate limiting step for initiating IL15 induced T cell proliferation.

In summary, we developed a novel method that can be used to produce milligram quantities of highly pure (> 95% monomeric protein) soluble recombinant IL15-scFv proteins using HEK293 mammalian cell system. This method has been tested for multiple variants of IL15 fusion proteins with success and thus, provides a reliable way to produce IL15 variants from mammalian cells while avoiding the tedious denature and refolding cycles when using *E. coli* system. Moreover, this method makes production of large amount of IL15 fusion proteins from mammalian cells possible without the need of tagging IL15Rα-sushi domain. By using sole IL15 as a functional domain, it provides freedom in designing more complex therapeutic drug formats, such as bispecific or trispecific molecules containing an IL15 domain, since the additional two disulfide bonds in IL15Rα-sushi domain may complex the productivity of these drug candidates due to higher risks of disulfide scrambling.

In addition, we also provided an answer to the loss of activities for some of IL15 fusion proteins. We found that the residue 112 of IL15 domain has a dramatic impact on $IL15_{K86R}$-A10m3 bioactivities, since the molecule size at this position may interfere with IL15 mediated γc signaling. Indeed, replacing Asparagine with Alanine improved the mutant's activity to the level comparable to WT hIL15. Lastly, we demonstrated that the residue 71 of IL15 domain is critical for IL15 mediated IL2β receptor signaling, which is a rate limiting step for T cell proliferation in response to IL15 stimulation.

## Conflicts of interest

None. All authors were employees of Sonnet Biotherapeutics when the study was carried out.

## Acknowledgment

We thank Zhihao Cui and Anil Bhate for excellent technical assistance and reading the manuscript. The project was solely supported by Sonnet Biotherapeutics.

## Appendix A. Supplementary data

Supplementary data related to this article can be found at http://dx.doi.org/10.1016/j.pep.2018.03.010.

## References

[1] J.A. Johnston, C.M. Bacon, D.S. Finbloom, R.C. Rees, D. Kaplan, K. Shibuya, J.R. Ortaldo, S. Gupta, Y.Q. Chen, J.D. Giri, J.J. O'Shea, Tyrosine phosphorylation and activation of STAT5, STAT3, and Janus kinases by interleukins 2 and 15, Proc. Natl. Acad. Sci. U.S.A. 92 (1995) 8705–8709.

[2] D.M. Anderson, S. Kumaki, M. Ahdieh, J. Bertles, M. Tometsko, A. Loomis, J. Giri, N.G. Copeland, D.J. Gilbert, N.A. Jenkins, V. Valentine, D.N. Shapiro, S.W. Morris,

L.S. Park, D. Cosman, Functional characterization of the human interleukin-15 receptor α a chain and close linkage of IL15RA and IL2RA genes, J. Biol. Chem. 270 (1995) 29862–29869.
[3] R. Meazza, S. Basso, A. Gaggero, D. Detotero, L. Trentin, R. Pereno, B. Azzarone, S. Ferrini, Interleukin (IL)-15 induces survival and proliferation of the growth factor-dependent acute myeloid leukemia M-07e through the IL-2 receptor β/γ, Int. J. Canc. 78 (1998) 189–195.
[4] M. Chirifu, C. Hayashi, T. Nakamura, S. Toma, T. Shuto, H. Kai, Y. Yamagata, S.J. Davis, S. Ikemizu, Crystal structure of the IL-15-IL15Rα complex, a cytokine-receptor unit presented *in trans*, Nat. Immunol. 8 (2007) 1001–1007.
[5] A.M. Ring, J.X. Lin, D. Feng, S. Mitra, M. Rickert, G.R. Bowman, V.S. Pande, P. Li, I. Moraga, R. Spolski, E. Ozkan, W.J. Leonard, K.C. Garcia, Mechanistic and structural insight into the functional dichotomy between IL-2 and IL-15, Nat. Immunol. 13 (2012) 1187–1195.
[6] X. Zhu, W.D. Marcus, W. Xu, H. Lee, K. Han, J.O. Egan, J.L. Yovandich, P.R. Rhode, H.C. Wong, Novel human Interleukin-15 agonists, J. Immunol. 183 (2009) 3598–3607.
[7] T.A. Waldmann, The shared and contrasting roles of IL2 and IL15 in the life and death of normal and neoplastic lymphocytes: implications for cancer therapy, Canc. Immunol. Res. 3 (2015) 219–227.
[8] B.M.K. Kennedy, M. Glaccum, S.N. Brown, E.A. Butz, J.L. Viney, M. Embers, N. Matsuki, K. Charrier, L. Sedger, C.R. Willis, K. Brasel, P.J. Morrissey, K. Stocking, J.C.L. Schuh, S. Joyce, J.J. Peschon, Reversible defects in natural killer and memory CD8 T cell lineages in interleukin 15-deficient mice, J. Exp. Med. 191 (5) (2000) 771–780.
[9] W. Xu, M. Jones, B. Liu, X. Zhu, C.B. Johnson, A.C. Edwards, L. Kong, E.K. Jeng, K. Han, W.D. Marcus, M.P. Rubinstein, P.R. Rhode, H.C. Wong, Efficacy and Mechanism-of-Action of a novel superagonist interleukin-15: interleukin-15 receptor α Su/Fc fusion complex in syngeneic murine models of multiple myeloma, Cancer Res. 73 (2013) 3075–3086.
[10] N.D. Huntington, The unconventional expression of IL-15 and its role in NK cell homeostasis, Immunol. Cell Biol. 92 (2014) 210–213.
[11] S.A. Rosenberg, Interleukin-2 and the development of immunotherapy for the treatment of patients with cancer, Canc. J. Sci. Am. 6 (Suppl. 1) (2000) S2–S7.
[12] W. Munger, S.Q. DeJoy, R. Jeyaseelan Sr., L.W. Torley, K.H. Grabstein, J. Eisenmann, R. Paxton, T. Cox, M.M. Wick, S.S. Kerwar, Studies evaluating the antitumor activity and toxicity of interleukin-15, a new T cell growth factor: comparison with interleukin-2, Cell. Immunol. 165 (1995) 289–293.
[13] T.A. Waldmann, E. Lugli, M. Roederer, L.P. Perera, J.V. Smedley, R.P. Macallister, C.K. Goldman, B.R. Bryant, J.M. Decker, T.A. Fleisher, H.C. Lane, M.C. Sneller, R.J. Kurlander, D.E. Kleiner, J.M. Pletcher, W.D. Figg, J.L. Yovandich, S.P. Creekmore, Safety (toxicity), pharmacokinetics, immunogenicity, and impact on elements of the normal immune system of recombinant human IL-15 in rhesus macaques, Blood 117 (2011) 4787–4795.
[14] K.C. Conlon, E. Lugli, H.C. Welles, S.A. Rosenberg, A.T. Fojo, J.C. Morris, T.A. Fleisher, S.P. Dubois, L.P. Perera, D.M. Stewart, C.K. Goldman, B.R. Bryant, J.M. Decker, J. Chen, T.A. Worthy, W.D. Figg Sr., C.J. Peer, M.C. Sneller, H.C. Lane, J.L. Yovandich, S.P. Creekmore, M. Roederer, T.A. Waldmann, Redistribution, hyperproliferation, activation of natural killer cells and CD8 T cells, and cytokine production during First-in-human clinical trial of recombinant human interleukin-15 in patients with cancer, J. Clin. Oncol. 33 (2015) 74–82.
[15] S. Hoefman, I. Ottevaere, J. Baumeister, M.L. Sargentini-Maier, Pre-clinical intravenous serum pharmacokinetics of albumin binding and non-half-life extended nanobodies, Antibodies 4 (2015) 141–156.
[16] K. Han, X. Zhu, B. Liu, E. Jeng, L. Kong, J.L. Yovandich, V.V. Vyas, W.D. Marcus, P.A. Chavaillaz, C.A. Romero, P.R. Rhode, H.C. Wong, IL-15:IL-15 receptor alpha superagonist complex: high-level co-expression in recombinant mammalian cells, purification and characterization, Cytokine 56 (2011) 804–810.
[17] A. Bessard, V. Sole, G. Bouchaud, A. Quemener, Y. Jacques, High antitumor activity of RLI, an interleukin-IL15 (IL-15)-IL-15 receptor α fusion protein, in metastatic melanoma and colorectal cancer, Mol. Canc. Therapeut. 8 (2009) 2736–2745.
[18] M.M. Schmidt, S.A. Townson, A.J. Andreucci, B.M. King, E.B. Schirmer, A.J. Murillo, C. Dombrowski, A.W. Tisdale, P.A. Lowden, A.L. Masci, J.T. Kovalchin, D.V. Erbe, K.D. Wittrup, E.S. Furfine, T.M. Barnes, Crystal structure of an HSA/FcRn complex reveals recycling by competitive mimicry of HSA ligands at a pH-dependent hydrophobic interface, Structure 21 (2013) 1966–1978.
[19] M.S. Dennis, M. Zhang, Y.G. Meng, M. Kadkhodayan, D. Kirchhofer, D. Combs, L.A. Damico, Albumin binding as a general strategy for improving the pharmacokinetics of proteins, J. Biol. Chem. 277 (2002) 35035–35043.
[20] A. Wunder, U. Muller-Ladner, E.H.K. Stelzer, J. Funk, E. Neumann, G. Stehle, T. Pap, H. Sinn, S. Gay, C. Fiehn, Albumin-based drug delivery as novel therapeutic approach for rheumatoid arthritis, J. Immunol. 170 (2003) 4793–4801.
[21] A. Ward, M. Anderson, R.I. Craggs, J. Maltby, C. Grahames, R.A. Davies, D. Finch, D. Pattison, H. Oakes, P.R. Mallinder, *E. coli* expression and purification of human and cynomolgus IL-15, Protein Expr. Purif. 68 (2009) 42–48.
[22] R.N. Bamford, A.P. DeFilippis, N. Azimi, G. Kurys, T.A. Waldmann, The 5' untranslated region, signal peptide, and the coding sequence of the carboxyl terminus of translational control, J. Immunol. 160 (1998) 4418–4426.
[23] C. Bergamaschi, M. Rosati, R. Jalah, A. Valentin, V. Kulkarni, C. Alicea, G.M. Zhang, V. Patel, B.K. Felber, N. Pavlakis, Intracellular interaction of interleukin-15 with its receptor α during production leads to mutual stabilization and increased bioactivity, J. Biol. Chem. 283 (2008) 4189–4199.
[24] R. Pereno, J. Giron-Michel, A. Gaggero, E. Cazes, R. Meazza, M. Monetti, E. Monaco, Z. Mishal, C. Jasmin, F. Indiveri, S. Ferrini, B. Azzarone, IL-15/IL15Rα intracellular trafficking in human melanoma cells and signal transduction through the IL15Rα, Oncogene 19 (2000) 5153–5162.
[25] E. Mortier, T. Woo, R. Advincula, S. Gozalo, A. Ma, IL-15Rα chaperones IL-15 to stable dendritic cell membrane complexes that activate NK cells via trans presentation, J. Exp. Med. 205 (2008) 1213–1225.
[26] V.V. Vyas, D. Esposito, T.L. Sumpter, T.L. Broadt, J. Hartley, I.V.G.C. Knapp, W. Cheng, M.S. Jiang, J.M. Roach, X. Yang, S.L. Giardina, G. Mitra, J.L. Yovandich, S.P. Creekmore, T.A. Waldmann, J. Zhu, Clinical manufacturing of recombinant human interleukin 15. I. production cell line development and protein expression in *E. coli* with stop codon optimization, Biotechnol. Prog. 28 (2012) 497–507.
[27] X.Q. Wei, M. Orchardson, J.A. Gracie, B.P. Leung, B.M. Gao, H. Guan, W. Niedbala, G.K. Paterson, I.B. McInnes, F.Y. Liew, The Sushi domain of soluble IL-15 receptor α is essential for binding IL-15 and inhibiting inflammatory and allogenic responses in vitro and in vivo, J. Immunol. 167 (2001) 277–282.
[28] S.H. Lecker, A.L. Goldberg, W.E. Mitch, Protein degradation by the ubiquitin-proteasome pathway in normal and disease states, J. Am. Soc. Nephrol. 17 (2006) 1807–1819.
[29] M. Kaspar, E. Trachsel, D. Neri, The antibody-mediated targeted delivery of interleukin-15 and GM-CSF to the tumor neovasculature inhibits tumor growth and metastasis, Cancer Res. 67 (2007) 4940–4948.
[30] M. Thaysen-Andersen, E. Chertova, C. Bergamaschi, E.S.X. Moh, O. Chertov, J. Roser, R. Sowder, J. Bear, J. Lifson, N.H. Packer, B.K. Felber, G.N. Pavlakis, Recombinant human heterodimeric IL-15 complex displays extensive and reproducible N- and O-linked glycosylation, Glycoconj. J. 33 (2016) 417–433.